

Preliminary Validation and Performance of the Jason Microwave Radiometer

Shannon Brown and Chris Ruf
University of Michigan
Ann Arbor, MI

Steve Keihm and Ami Kitiyakara
Jet Propulsion Laboratory
Pasadena, CA

Abstract – The Jason Microwave Radiometer is calibrated using hot and cold on-Earth theoretical brightness temperature references. The retrieved path delay values are validated using co-located Topex Microwave Radiometer and radiosonde values. The calibrated path delay values are demonstrated to have no significant bias or scale errors. The absolute accuracy of the individual path delay measurements exceeds the mission goal of 1.2 cm RMS.

Keywords–calibration; microwave radiometer; JMR; TMR; satellite; path delay

I. INTRODUCTION

The Jason Microwave Radiometer (JMR) is an instrument flying on the Jason-1 radar altimetry satellite. Jason-1, which is designed to produce global maps of ocean surface topography, is a joint venture by NASA and the French space agency Centre National d'Etudes Spatiales (CNES). It was launched on December 7, 2001 from Vandenberg Air Force Base. JMR is included to measure the electrical range delay (referred to as path delay) of the altimeter signal through the troposphere due to water vapor and cloud liquid water. If the path delay in the altimeter signal is left uncorrected, the errors in the altimeter range measurement will be on the order of 3 – 45 cm [1]. JMR operates at 18.7, 23.8, and 34.0 GHz with a nadir viewing geometry and 1-second integration time [2]. The Jason-1 mission is a follow-on to the highly successful Topex/Poseidon (T/P) mission, which was launched on August 10, 1992. The Topex Microwave Radiometer (TMR) has been determining the wet path delay correction of the atmosphere to the 1.1 cm level of accuracy for over 10 years [3]. JMR is required to retrieve the wet tropospheric path delay with an RMS accuracy of 1.2 cm with the goal of 1.0 cm. For calibration purposes, Jason was placed in an identical orbit as T/P, with only a ~70 second displacement, for the first 8 months of the mission.

The JMR calibration approach is divided into two parts. The first part is the calibration of the brightness temperatures (TBs) at the coldest and hottest ends of the TB dynamic range. For the three JMR channels, this range is approximately 120 – 310 K. The TBs at the cold end are calibrated using a vicarious cold reference temperature at each frequency [4]. The TBs are calibrated at the hot end using approximate blackbody reference targets over the Amazon rainforest [5]. The second part is the validation of the path delay values which are retrieved from the TB measurements. The JMR PD values are compared to time and space co-incident radiosonde (RaOb) derived refractivity profiles and to TMR PD values. Due to the co-tracking orbits, there is negligible time or space decorrelation when comparing PDs between JMR and TMR,

thus it affords unprecedented accuracy in the intercalibration between the two instruments. It is essential that there be no significant bias (i.e., offset error) between the JMR and TMR PDs. This will ensure continuity in the water vapor corrections provided to the TOPEX and Jason Range measurements. It is also essential that there be no significant scale error in the JMR PD retrieval, since an error that scales with path delay can cause errors in the ocean height retrieval that are spatially correlated over large distances.

The JMR TB calibration was adjusted by changing three sets of coefficients in the calibration processing algorithms. The off Earth side lobe fractions were adjusted in the antenna pattern correction (APC) algorithm and the front end loss coefficients and the noise source gain in the antenna temperature calibration algorithm were adjusted to meet the calibration criteria.

II. BRIGHTNESS TEMPERATURE CALIBRATION RESULTS

A. Comparisons with the vicarious cold reference

The vicarious cold reference represents a statistical lower bound on brightness temperature for a given frequency [4]. It is found by forming a cumulative distribution function of the coldest TBs, then extrapolating to a zero-probability. This gives the warmest TB that has a zero probability of occurring. The theoretical cold reference value for each frequency is dependent on the model chosen for the sea surface emission. The theoretical cold reference difference between two frequencies is largely model independent. Thus the cold reference difference between the adjacent JMR and TMR channels is used as the calibration reference. The theoretical value is determined by applying a radiative transfer model to RaOb profiles from 59 open ocean island sites. The Stogryn 1971 [6] sea water dielectric model is used with an updated version of the Liebe 1987 [7] atmospheric water vapor absorption model and the Rosenkranz 1993 [8] oxygen absorption model to determine the brightness temperature from the RaOb profiles for JMR and TMR frequencies. The theoretical cold reference differences are given in Table I. The results of the JMR – TMR cold reference differences after the calibration coefficients were adjusted are given in Table II. The JMR-TMR TBs at the cold end are in good agreement with the theoretical values for cycles 3 - 20.

TABLE I. THEORETICAL VICARIOUS COLD REFERENCE TB DIFFERENCES

18.7 – 18.0 GHz	1.51 K ± 0.30
23.8 – 21.0 GHz	3.11 K ± 1.2
34.0 – 37.0 GHz	-5.61 K ± 0.20

TABLE II. JMR – TMR VICAROUS COLD REFERENCE TB DIFFERENCES (CYCLES 3 – 20)

JMR 18.7 – TMR 18.0	1.60 K ± 0.28
JMR 23.8 – TMR 21.0	4.02 K ± 0.58
JMR 34.0 – TMR 37.0	-6.09 K ± 0.32

B. Comparison with the hot reference

The method to determine the hot reference temperature is given in [5]. The method essentially transfers the calibration of SSM/I to JMR over two approximate blackbody regions in the Amazon Rainforest. Two regions are used where the vegetation is optically thick; therefore the surface emission is independent of polarization and incidence angle. Region 1 is 5° – 10° S and 65° – 74° W and region 2 is 1° S – 4° N and 53° – 59° W. The TBs at SSM/I frequencies and incidence are transferred to JMR frequencies and incidence and using several relationships that are parameterized from a radiative transfer model. Table III gives the hot reference TB values for days 34 – 230 of 2002 from SSM/I F13, F14, and F15 platforms. Table IV gives the corresponding JMR average values for the same time of year after the final calibration adjustments.

III. PATH DELAY VALIDATION

A. Comparison with TMR

The offset between the co-located JMR and TMR PDs is used to validate the retrieved JMR PD values. Fig. 1 shows the pass averaged JMR – TMR PD deltas for cycles 3 – 20 after the final calibration adjustments. The plot is divided into low (JMR PD < 10 cm), medium (10 < PD < 20 cm), and high (PD > 20 cm) bins. There is a negligible residual offset for all of the PD ranges. Table V is a summary of the mean and RMS of the PD deltas for cycles 3 – 20. The RMS error between the JMR and TMR PDs can be completely explained by the uncorrelated sources of error between the two instruments. This means that the absolute accuracy of the JMR PDs is at least as good as the TMR PDs, which have a demonstrated RMS accuracy less than 1.1 cm [9].

TABLE III. JMR AMAZONIA HOT REFERENCE MODEL TEMPERATURES

Hot Reference TBs	Region 1 (K)	Region 2 (K)
18.7 GHz	286.4491	286.8298
23.8 GHz	285.4591	285.4619
34.0 GHz	282.3796	282.6957

TABLE IV. AVERAGE MEASURED JMR TBs OVER AMAZONIA REFERENCE REGIONS (CYCLES 3 – 20)

JMR Hot TBs	Region 1 (K)	Region 2 (K)
18.7 GHz	284.4887	285.4608
23.8 GHz	284.5535	285.4623
34.0 GHz	281.3733	282.4813

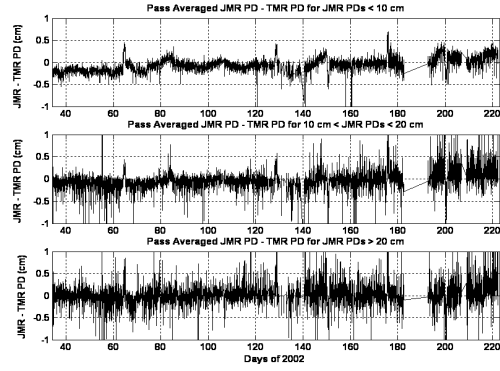


Figure 1. Pass averaged JMR – TMR path delays for low, medium, and high PD bins shown for JMR cycles 3 – 20.

TABLE V. PASS-AVERAGED JMR – TMR PATH DELAY DIFFERENCE AND RMS FOR CYCLES 3 – 20

JMR – TMR Path Delay	Mean (cm)	RMS (cm)
PD < 10 cm	-0.050	0.435
10 cm > PD < 20 cm	-0.035	0.429
PD > 20 cm	0.019	0.575
All PDs	-0.021	0.488

B. Comparison with Radiosondes

The JMR PDs are also validated using path delays derived from radiosonde humidity profiles of the atmosphere. JMR is required to accurately retrieve the path delay under windy and cloudy conditions. The all weather JMR performance can be assessed by using the integrated liquid water and surface wind speed estimations that are derived from JMR TBs. The accuracy of the liquid water and wind speed estimations has not been independently validated for this study, but is adequate to separate the data into different weather groups. The RMS accuracy and mean JMR – RaOb PD differences are shown in Table VI for various cloud and wind conditions, as well as various spatial and temporal bounds. The mean bias is 0.46 cm with a RMS accuracy of 3.17 cm for all conditions, with 315 km and 6 hours as the bounds on the closest approach point. The closest approach point is defined as the JMR measurement that has a minimum spatial and temporal separation from the RaOb launch. The mean bias and RMS accuracy both improve as the closest approach point bounds become tighter. The RMS accuracy of the retrieval is also not affected by varying cloud or wind conditions.

The RMS error between the JMR and RaOb PDs is a function of the error in the RaOb humidity measurements, the spatial and temporal decorrelation between the two points, and the error in the JMR PD retrieval.

$$RMS_{JMR - RaObPD} (dist, time) = [\Delta RaOb^2 + \Delta JMR^2 + \Delta Spatial (dist)^2 + \Delta Temporal (time)^2]^{1/2} \quad (1)$$

TABLE VI. COMPARISON OF JMR PATH DELAYS WITH TIME AND SPACE COINCIDENT RADIOSONDE PROFILES FOR VARIOUS CLOSEST APPROACH POINTS AND VARIOUS WEATHER CONDITIONS

Integrated Liquid Water (μm)	Surface Wind (m/s)	Spatial Separation (km)	Temporal Separation (hrs)	Mean (cm) JMR - RaOb	RMS (cm) JMR - RaOb	Number of Samples
<i>ALL Liquid</i>	<i>All Wind</i>	< 315	≤ 6	0.46	3.17	1109
<i>ALL Liquid</i>	<i>All Wind</i>	< 150	≤ 3	0.25	2.65	183
<i>ALL Liquid</i>	<i>All Wind</i>	< 75	≤ 1	-0.20	1.90	40
< 100	<i>All Wind</i>	< 315	≤ 6	0.37	3.17	884
100 < liq < 300	<i>All Wind</i>	< 315	≤ 6	0.76	3.02	178
> 300	<i>All Wind</i>	< 315	≤ 6	1.07	3.73	47
<i>ALL Liquid</i>	< 7	< 315	≤ 6	0.16	3.23	610
<i>ALL Liquid</i>	7 < wind < 15	< 315	≤ 6	0.83	3.11	481
<i>ALL Liquid</i>	> 15	< 315	≤ 6	1.13	3.42	18

The absolute accuracy of JMR can be estimated by extrapolating to zero separation the dependence of the RMS difference between JMR and RaOb PDs on spatial and temporal separation. The extrapolated value, determined from Fig. 2, is $1.0 \text{ cm} \pm 0.6 \text{ cm}$. This is an upper bound on the JMR accuracy, assuming ideal RaOb measurements.

IV. CONCLUSIONS

Results are presented from the calibration of JMR TBs and validation of the PDs. The TBs are shown to be in agreement with theoretical cold and hot TB reference values. The path delay retrieval is shown to have a near zero offset from corresponding TMR PDs and negligible scale error. The 1-second JMR PD measurements are estimated to have an RMS accuracy of better than 1.2 cm, thus satisfying the mission requirement.

V. REFERENCES

- [1] S. Keihm, M. Janssen, and C. Ruf, "TOPEX/POSEIDON microwave radiometer (TMR), III, Wet troposphere range correction algorithm and pre-launch error budget," IEEE Trans. Geosci. Remote Sens., vol. 33, 1, pp. 147 – 160. Jan. 1995.
- [2] Jason-1 Project, Oct. 2001, "AVISO and POCAAC User Handbook IGDR and GDR Jason Products," Edition 1.0, JPL D-21352 (PODAAC)
- [3] C. Ruf, S. Keihm, B. Subramanya, and M. Janssen, "TOPEX/POSEIDON microwave radiometer performance and in-flight calibration," J. of Geo. Res, vol. 99, C12, pp. 24,915 – 24,926, Dec. 1994.
- [4] C. Ruf, "Detection of Calibration Drifts in Spaceborne Microwave Radiometers Using a Vicarious Cold Reference," IEEE Trans. On Geosci. Remote Sens, vol. 38, 1, Jan. 2000.
- [5] S. Brown and C. Ruf. "Determination of a Hot Blackbody Reference Target over the Amazon Rainforest for the On-orbit Calibration of Microwave Radiometers," unpublished.
- [6] A. Stogryn, "Equations for calculating the Dielectric Constant of Saline Water," IEEE Trans on Microwave Theory and Techniques, pp. 733-736, 1971
- [7] S. Cruz Pol, C. Ruf, and S. Keihm, "Improved 20-32 GHz atmospheric absorption model," Radio Sci., vol 22, 5, pp. 1319-1333, 1998.
- [8] P. Rosenkranz, "Absorption of Microwaves by Atmospheric Gases," Atmospheric Remote Sensing by Microwave Radiometry, Chapter 2 Ed. By Janssen, Wiley, New York, 1993.
- [9] S. Keihm, V. Zlotnicki, and C. Ruf, "TOPEX Microwave Radiometer performance evaluation 1992-1998," IEE Trans on Geosci and Remote Sens., vol 38, no 3, pp 1379-1386, 2000.

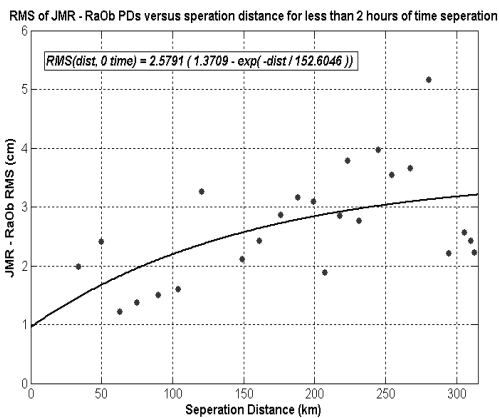


Figure 2. RMS error between the JMR and RaOb Path Delays as a function of spatial separation for measurements with less than 2 hours of time separation.